

## The Evaluations of NEX-GDDP and Marksim Downscaled Data Sets Over Lali Region, Southwest Iran

Zeydalinejad, N.<sup>1</sup>, Nassery, H. R.<sup>2\*</sup>, Shakiba, A. R.<sup>3</sup> and Alijani, F.<sup>4</sup>

1. Ph.D. Student, Department of Mineral Geology and Hydrogeology, Faculty of Earth Sciences, Shahid Beheshti University, Tehran, Iran

2. Professor, Department of Mineral Geology and Hydrogeology, Faculty of Earth Sciences, Shahid Beheshti University, Tehran, Iran

3. Associate Professor, Department of Remote Sensing and GIS, Faculty of Earth Sciences, Shahid Beheshti University, Tehran, Iran

4. Assistant Professor, Department of Mineral Geology and Hydrogeology, Faculty of Earth Sciences, Shahid Beheshti University, Tehran, Iran

(Received: 8 Jan 2020, Accepted: 9 June 2020)

### Abstract

Downscaling of climatic variables is a difficult problem in the climate change impact studies. However, some climatic data sets exist that have been universally downscaled. These data sets introduce climatic data even in regions with scarce observations. In this study, NASA Earth Exchange Global Daily Downscaled Projections (NEX-GDDP) and Markov simulation (Marksim) downscaled data sets were evaluated over Lali region, southwest Iran by comparing the monthly RMSE, average and variance differences between the observation data and General Circulation Models' (GCMs') outputs during the time period 2010-2016. The NEX-GDDP data set contains 21 GCMs under two Representative Concentration Pathways (RCPs), i.e. RCP4.5 and RCP8.5, from 1951 to 2099, and the Marksim data set includes 17 GCMs under all RCPs from 2010 to 2095. Results acknowledged the ability of both data sets in projecting the climatic variables in the study area. Finally, NorESM1-M and GFDL-CM3 depicted the best operation for precipitation and temperature, respectively.

**Keywords:** NEX-GDDP, Marksim, GCM, Lali region, RCP.

### 1. Introduction

Downscaling of General Circulation Models' (GCMs') outputs is demanding and time-consuming. Fortunately, some climatic data sets such as NASA Earth Exchange Global Daily Downscaled Projections (NEX-GDDP) and Markov simulation (Marksim) exist. These data sets are attainable globally in both spatial and temporal downscaled types. However, whether they can be applied in a small-scale region, i.e. over a synoptic station, is a question. If they can, a difficulty can be solved, especially for the regions like the Middle East where little observations are accessible. Further, they can provide a basis for comparing the climate change impact studies since they have been produced by the same approach in the global scale.

Sophisticated storylines are employed to project the future greenhouse gas concentrations and climate change in a specific time period (IPCC, 2013). GCMs are applied to achieve this purpose, and downscaling techniques overcome the coarse resolution of the outputs (Wilby and Wigley,

1997). Until recently, climate change impact studies have been carried out under the previous climate change scenarios represented by the Intergovernmental Panel on Climate Change (IPCC) in the Fourth Assessment Report (AR4) entitled as the Special Report on Emission Scenarios (SRES). However, IPCC (2014) introduced Representative Concentration Pathways (RCPs) in the Fifth Assessment Report (AR5). Specifically, RCPs are the trajectories of greenhouse gas concentrations (Ma et al., 2016) related to the greenhouse gases, aerosols, ozone, land use and land cover changes in the future; however, the previous scenarios only encompassed forcing of the greenhouse gases and aerosols (Meinshausen et al., 2011). Newer scenarios, i.e. RCPs, have improved the representation of the real world due to including the projections of greenhouse gases time-dependently (Taylor et al., 2012). Indeed, IPCC answered disparate scientific vicissitudes relating to the projection of the climate for the newer

\*Corresponding author:

h-nassery@sbu.ac.ir

scenarios at Coupled Model Intercomparison Project Phase 5 (CMIP5) (Chen et al., 2014; Ul Hasson et al., 2016). Depending on the radiative forcing at the end of the 21<sup>st</sup> Century, RCPs were categorized as RCP2.6, RCP4.5, RCP6 and RCP8.5 (Ma et al., 2016). The interested readers may consult the related resources such as Chaturvedi et al. (2012), Chou et al. (2014), Jones and Thornton (2013), Ma et al. (2016), Meinshausen et al. (2011), and Semenov and Stratonovitch (2015) to gain more detailed information regarding the RCPs.

McSweeney et al. (2015) analyzed the CMIP5 GCMs in southeast Asia, Europe and Africa to select the best GCMs. They nominated three models, i.e. MIROC-ESM, MIROC-ESM-CHEM and IPSL-CM5B-LR as “implausible.” Bao and Wen (2017) applied the NEX-GDDP data set to project the near- and long-term future climate over China by means of representing it as a new downscaled data set with extremely high resolution that reduces the biases of GCMs and with the potential to be widely employed in the future. Daksiya et al. (2017) investigated the maximum daily precipitation for Jakarta, Indonesia in the future time period using three downscaling techniques, i.e. LARS-WG, SDSM and NEX-GDDP, by considering different models and scenarios. As they mentioned, the problem with LARS-WG is that it does not take the newer scenarios. Even though it has been applied in studies such as Semenov and Stratonovitch (2015) and Ma et al. (2016) for the newer scenarios, its ultimate version, i.e. LARS-WG6.0, is undergoing some experiments. On the other hand, SDSM just involve one GCM, i.e. CanESM2, for the newer scenarios. Therefore, they utilized the third approach, i.e. the NEX-GDDP data set. The results depicted enhancing of about 20 percent of the daily precipitation maxima for the region in the future time period. Chen et al. (2017) assessed the future precipitation extreme events in China by means of the NEX-GDDP data set and introduced it as a new downscaled data set with high resolution. Moreover, the ability of the data set in projecting the precipitation extreme events and long-term climate change was evaluated, and its power was compared with the CMIP5 GCMs' outputs. The study

denoted the great competence of the data set in projecting the spatial patterns of the precipitation extreme events over China. In comparison with the GCMs' outputs, the NEX-GDDP data set's outputs demonstrated more resemblance to the observation data, higher Pearson's correlation, less relative errors and uncertainty; moreover, the NEX-GDDP data set introduced more details at local to regional scale. Therefore, they prognosticated this data set, especially for climate change impact studies in local scales, would probably achieve more popularity in the future. Jones and Thornton (2013) represented Marksim as a prevalent downscaling procedure to produce daily downscaled climate data for an ensemble of GCMs and different scenarios. Its development had taken more than 20 years and as the producers predicted its power has been ascended by including more calibration stations and newer scenarios in its new (web) version. In a study by Jones and Thornton (2013), 73 precipitation stations, including numerous precipitation situations, were deemed worldwide. The results depicted Marksim could estimate the precipitation accurately so that the variances of the observed and simulated precipitation data demonstrated minimal differences. However, the higher errors were approximately related to the colder climates.

GCMs are not capable of taking into account the hydrological processes, which typically occur at the finer scales (Kundzewicz et al., 2007). Indeed, due to some imperatives accompanied by manifold statistical approaches and computer programs, climate change impact studies have been restricted to some specific sites and climatic scenarios (Wilby et al., 2004). Learning and applying downscaling approaches are challenging and time-consuming for researchers, especially those with restrictive statistical and programming virtuosity. Moreover, IPCC introduces new assessment reports every few years, and therefore, not only would the GCMs be obsolescence but also emission scenarios would change so that the regression equations or transmission functions are contemporized to downscale the GCMs' outputs. Additionally, even though the observation data, at least for several synoptic stations, are required for the regional and

national projects, for regions over than the USA, especially for the developing countries, it is often difficult to obtain access to the synoptic observation data, especially during the recent decades (Funk et al., 2010); however, the accuracy of the selected downscaling method in simulating the climatic variables should be verified. Even though the satellite technology is being developed and it can measure some aspects of climate and weather, it cannot be taken into account as a surrogate for the field observations. Furthermore, the output format of the GCMs is not always in a type to be directly employed in the hydrological models. Therefore, an outstanding process must be done on this data format before using it in a meaningful way. This process may include the spatial and temporal downscaling of the GCMs' outputs (Jones and Thornton, 2013).

Different downscaling approaches with the advantages and disadvantages exist so that every approach is appropriate for a specific purpose (Wilby et al., 2009). Downscaling approaches have uncertainties. By considering the GCMs' outputs, it is obvious that climate change projections are not analogous everywhere during the past and future time periods. In other words, no coincidence exists between the GCMs for some regions (Wilby, 2007). Many uncertainties exist in relation to the tropical storms and regional precipitation patterns in most parts of Africa, Southern Asia and Latin America so that considering different scenarios and GCMs, especially for these regions, are recommended. Moreover, assessing the local impacts of climate change is not always adequate, and evaluating the uncertainty of different downscaling approaches is challenging. Additionally, information of the near future (3-20 years) does not exist (Washington et al., 2006). However, using the outputs of GCMs that have been already verified by the observation data sets is a quick way to achieve the downscaled climate data (Trotochaud et al., 2016). Being globally applicable and requiring few inputs are the main benefits of these data sets.

Even though the computing processes are not identical in the NEX-GDDP and Marksim data sets, some similarities exist such that they can be compared. They include some analogous GCMs and emission scenarios, i.e. RCP4.5 and RCP8.5, with the same temporal and spatial resolutions; they include outputs with the same time period of 2010-2095; they have been downscaled by the statistical downscaling approach; and finally, they are globally downscaled and have been verified and re-evaluated many times.

Even though some studies exist that evaluate the climatic downscaled data sets, few studies that have assessed their operation over a small-scale region, i.e. over a synoptic station. In this study, firstly, the methodology utilized in producing the NEX-GDDP and Marksim data sets is represented. Then, the uncertainty of the NEX-GDDP and Marksim data sets for both RCP4.5 and RCP8.5 scenarios are evaluated over the Lali region, southwest Iran for the time period 2010-2016. Even though these data sets are downscaled globally, it is better to evaluate their uncertainties. Finally, not only the better data set selected but also the GCMs with the lowest uncertainties are selected so that climate change would be projected with sufficient accuracy during the future time period (2021-2050) in relation to the present time period (1961-1990).

## 2. Material and Methods

The Lali region is located in the north of Khuzestan Province, southwest Iran (Figure 1). Daily observation data of the Lali synoptic station, which is only available for the time period 2007-2016, was gathered from Iran Meteorological Organization (2018). The average temperature and precipitation are 25.11°C and 396 mm/year, respectively, for the time period 2007-2016. According to de Martonne climatic aridity index, the Lali climate type is semi-arid.

The NEX-GDDP and Marksim data sets are available online at <https://cds.nccs.nasa.gov/nex-gddp> and <http://gisweb.ciat.cgiar.org/MarkSimGCM>, respectively.

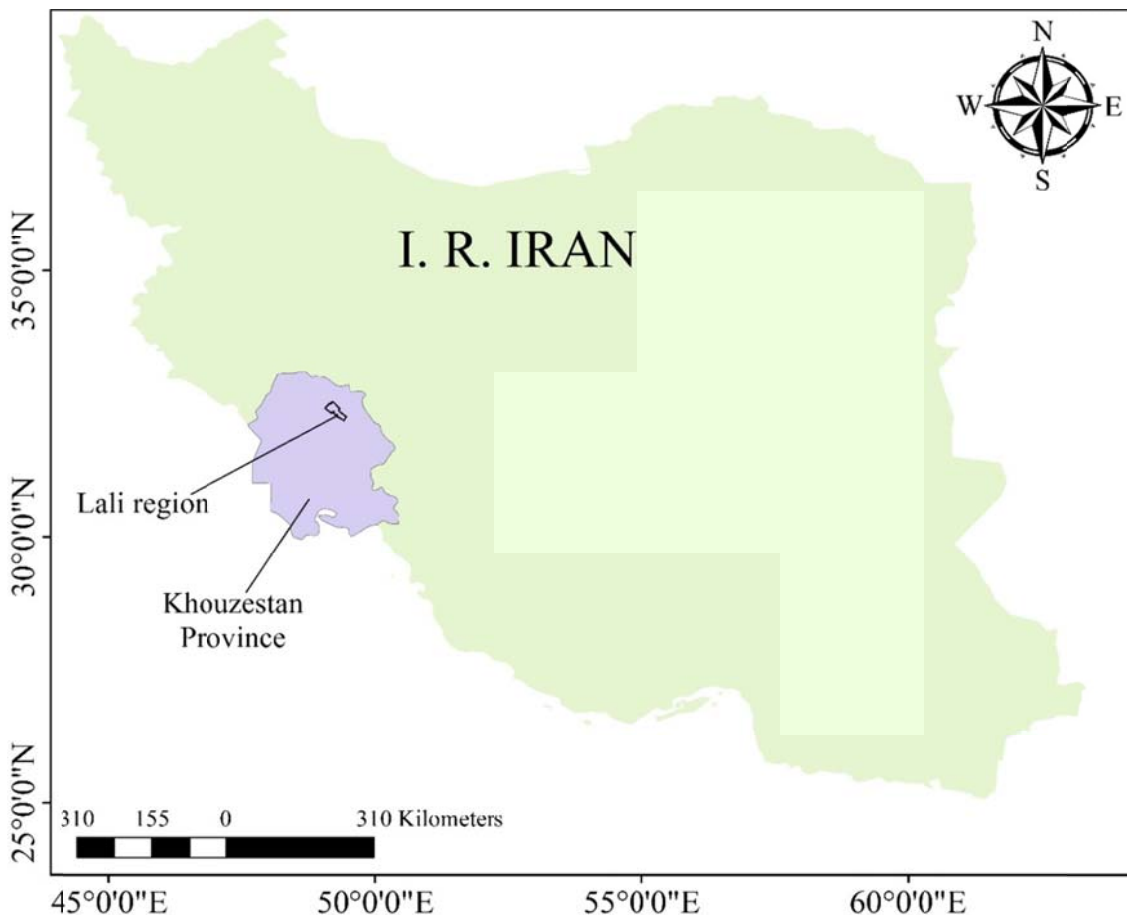


**Figure 1.** The location of Lali study area.

The present/historical time period and future time periods were deemed as 1961-1990 and 2021-2050, respectively. The Marksim data set includes data since 2010, therefore, 2010-2016 were considered as the verification time period. Moreover, the RCPs included in the NEX-GDDP, i.e. RCP4.5 and RCP8.5, were taken into account. The NEX-GDDP and Marksim data sets include 21 and 17 GCMs, respectively (Table 1). Twelve identical GCMs exist in both NEX-GDDP and Marksim data sets (Table 1). Not only the common models were considered and compared whether alone or as an ensemble, but also the outputs of the other models were assessed to have a total view of all GCMs involved in both data sets.

In recent regional to local scale climate change studies, the NEX-GDDP data set has been employed widely (Bao and Wen, 2017; Chen et al., 2017). Introducing bias-corrected and high-resolution climate change

projections that considers the topographic impacts has been the purpose of producing this data set (Thrasher et al., 2012). In other words, the topographic impacts influencing the local precipitation events have been deemed in the data set (Bao and Wen, 2017). Bias-Correction Spatial Disaggregation (BCSD) approach utilized in the NEX-GDDP data set is an algorithm or a statistical downscaling that makes the averages and variances of the GCMs' outputs and local observations as similar as viable (Maurer and Hidalgo, 2008; Thrasher et al., 2012; Wood et al., 2004). The method compares the GCMs' outputs and the corresponding climatic observation data, and then, the future climatic projections would be adjusted by the derived data so that more correlation would be achieved. The algorithm additionally interpolates the GCMs' outputs into the grids with higher resolutions using the derived spatial data.

**Table 1.** The details of GCMs involved in the NEX-GDDP (Thrasher and Nemani, 2015) and Marksim (<http://gisweb.ciat.cgiar.org/MarkSimGCM/docs/doc.html>) data sets.

Common GCMs involved in the NEX-GDDP and Marksim data sets		
Model name	Modelling center	Atmospheric resolution (lat×lon)
BCC-CSM1-1	Beijing Climate Center, China Meteorological Administration	2.8125×2.8125°
CSIRO-MK3-6-0	Common wealth Scientific and Industrial Research Organization in collaboration with the Queensland Climate Change Centre of Excellence	1.850×1.875°
GFDL-CM3	NOAA/Geophysical Fluid Dynamics Laboratory, US	2×2.5°
GFDL-ESM2G	NOAA/Geophysical Fluid Dynamics Laboratory, US	2×2.5°
GFDL-ESM2M	NOAA/Geophysical Fluid Dynamics Laboratory, US	2×2.5°
IPSL-CM5A-LR	L'Institut Pierre-Simon Laplace (IPSL), France	1.875×3.75°
IPSL-CM5A-MR	L'Institut Pierre-Simon Laplace (IPSL), France	1.25874×2.5°
MIROC5	Center for Climate System Research, National Institute for Environmental Studies, and Frontier Research Center for Global Change, Japan	1.40625×1.40625°
MIROC-ESM	National Institute for Environmental Studies, The University of Tokyo, Japan	2.8125×2.8125°
MIROC-ESM-CHEM	National Institute for Environmental Studies, The University of Tokyo, Japan	2.8125×2.8125°
MRI-CGCM3	Meteorological Research Institute, Japan	1.125×1.125°
NorESM1-M	Norwegian Climate Centre	1.875×2.5°
GCMs only involved in the NEX-GDDP data set		
Model name	Modelling center	Atmospheric resolution (lat×lon)
ACCESS1-0	Commonwealth Scientific and Industrial Research Organization and the Bureau of Meteorology, Australia	1.25×1.875°
BNU-ESM	College of Global Change and Earth System Science, Beijing Normal University	2.8×2.8°
CanESM2	Canadian Center for Climate Modelling and Analysis	2.8×2.8°
CCSM4	National Center for Atmospheric Research, US	0.9375×1.25°
CESM1-BGC	Community Earth System Model Contributors	0.9×1.25°
CNRM-CM5	Centre National de Recherches Météorologiques (CNRM), France	1.40625×1.40625°
INM-CM4	Institute for Numerical Mathematics	1.5×2°
MPI-ESM-LR	Max Planck Institute for Meteorology, Germany	1.875×1.875°
MPI-ESM-MR	Max Planck Institute for Meteorology, Germany	1.875×1.875°
GCMs only involved in the Marksim data set		
Model name	Modelling center	Atmospheric resolution (lat×lon)
BCC-CSM 1.1(m)	Beijing Climate Center, China Meteorological Administration	2.8125×2.8125°
FIO-ESM	The First Institute of Oceanography, SOA, China	2.8125×2.8125°
GISS-E2-H	NASA Goddard Institute for Space Studies	2×2.5°
GISS-E2-R	NASA Goddard Institute for Space Studies	2×2.5°
HadGEM2-ES	Met Office Hadley Centre	1.2414×1.875°

The NEX-GDDP data set includes precipitation and temperature projection for the retrospective period of 1951-2005 and prospective period of 2006-2099, as mentioned for 21 GCMs under the newer scenarios, involving medium-low (RCP4.5) and high (RCP8.5) emission scenarios, with the spatial resolution of 25° (25 km × 25 km) (Meinshausen et al., 2011; Taylor et al., 2012; Thrasher and Nemani, 2015). During

the downscaling process, the simulated retrospective data have been utilized as the training data so that they have been compared with the observation data. Then, the calculated relationships have been employed for downscaling of the prospective climatic projections. Indeed, all 42 climatic projections related to 21 GCMs and two RCPs have been downscaled similarly. Global Meteorological Forcing Data set

(GMFD) is employed for modeling the surface of the Earth, which is available at Terrestrial Hydrology Research Group, Princeton University (Sheffield et al., 2006). This data set combines the observation and reanalysis data, and it is available at the spatial resolutions of 0.25, 0.5 and 1 degrees and time steps of three-hourly, diurnal and monthly. After the bias-correction stage, which corrects the bias of the GCMs' outputs by making a comparison between the outputs and GMFD, the monthly climatic trends of data have been extracted. These trends are preserved in the corrected data and therefore, the probable statistical biases, especially the variances of the GCMs are corrected. At the spatial disaggregation stage, the corrected GCMs data is interpolated into the GMFD data grid with a resolution of 0.25°. Moreover, the relative spatial patterns of precipitation and temperature during the retrospective period are preserved in the future climate change. Finally, the frequency of the time periods with precipitation or temperature anomalies is maintained the same.

The Marksim data set is a third-order Markov chain weather simulator that is capable of predicting the occurrences of the wet days (Jones and Thornton, 2013). Developed during the last 20 years, Marksim introduces the GCMs' data for the time period 2010-2095 (Trotochaud et al., 2016). It is based on the WorldClim data set, which includes the observational weather data of the National Oceanic and Atmospheric Administration (NOAA), National Climate Data Center (NCDC) and Global Historical Climatology Network (GHCN). Marksim employs the stochastic downscaling and climatic grouping approaches to downscale the projections of the GCMs (Hijmans et al., 2005).

Both Marksim's web and software versions are similar; however, the interfaces differ. A user-friendly web version of Marksim is available, which introduces whether singular or every combination of the GCMs' simulations. The user is capable of defining the repetition number for the reproduction of the climatic data, i.e. precipitation, the minimum and maximum temperatures, and the solar radiation. The output data is in the diurnal time step for a specific year.

According to personal communication with Jones, Peter G. Marksim can simulate the time period 2021-2050 by selecting the year 2035 and repetition number 30. Finally, Random number seed is the initial value provided to the generator. Marksim downscales the future data through calibrating the GCMs' outputs for the 20<sup>th</sup> century in relation to the WorldClim data by means of the Markov chain regression (Jones and Thornton, 2013) and then, applying the developed regression models to the GCMs for the 21<sup>st</sup> century.

In relation to the present/historical time period, GCMs involved in Marksim have been run for the past 50-100 years. The GCMs' outputs have been modeled pixel by pixel by the polynomial regression approach. A data gap exists for the time period 1985-2010. No data exist for the years beyond 2095 because an extrapolation approach, which causes an extra error, would be required. An interpolation process has been carried out to convert the energy between the enormous atmospheric columns with low resolution (1-2°) and the finer ones. Moreover, the differences between the predictands of the future and base time periods are settled. In other words, a fifth-order polynomial function is correlated to the pixels of the GCMs to produce a time trend and then, the interpolation is applied to a finer grid. Finally, a third-order Markov chain with an autoregressive estimation downscales data to daily time steps. When using an ensemble of GCMs, Marksim utilizes the average of the polynomial functions. In relation to downscaling, the methodology involves reanalyzing the average differences between the observation data of synoptic stations and pixels or atmospheric columns of the GCMs' outputs; therefore, a statistical relationship is produced. A spatial downscaling is additionally applied by an interpolation considering 16 nodes surrounding the cell. Marksim takes into account 720 climate types all over the world to calculate the precipitation generator coefficients of third-order Markov. Weather typing is an aspect of Marksim that employs the most resembling climate in the world for a changing climate; however, new climates cannot be modeled. When the initial conditions change during

simulation, not only does the regression may modify but also the climate may differ. When GCMs' differentials exceed the Marksim's climate types, the algorithm extrapolates the most similar current climate type. The longer the simulation, the more probable would be to encounter this plight (Jones and Thornton, 2013). According to Jones, Peter G. Marksim (personal communication) deems 45000 observation synoptic stations globally, and 9600 climatic stations have been utilized in the calibration stage. Even though, the third-order Markov chain has been employed for simulating the precipitation, Marksim estimates the minimum and maximum temperatures using the SIMMETEO approach (Geng et al., 1988). Actually, WorldClim, which includes data in the time period 1961-1990 for most stations, represents the current climate; the method utilized in the WorldClim data is the same as Hutchinson (1997). Finally, after the calibration, some stations including different climatic types have been simulated for verification.

In this study, the statistical criteria are the Root Mean Square Error (RMSE), the monthly average differences and the monthly variance differences between the GCMs' outputs and the observation data. The RMSE equation is:

$$RMSE = \sqrt{\frac{\sum_{i=1}^N (O_i - P_i)^2}{N}} \quad (1)$$

where  $O_i$  and  $P_i$  are the observed and

simulated values for the  $i^{\text{th}}$  condition (Mohanty et al., 2015). The lower the RMSE, the more ability of the model to simulate.

### 3. Results

The monthly-average precipitation, minimum temperature and maximum temperature in the Lali region during the verification time period are 33.84 mm, 18.41°C and 31.89°C, respectively (Table 2). Tables 3 and 4 illustrate the RMSE, the average and variance differences between the GCMs' outputs and observation data for precipitation, the minimum and maximum temperatures considering all GCMs involved in the NEX-GDDP and Marksim data sets under RCP4.5 and RCP8.5, respectively, during the verification time period.

In relation to precipitation, the Marksim's GCMs demonstrate lower RMSE and average differences, and higher variance differences than the NEX-GDDP GCMs. Both data sets illustrate fewer amounts of RMSE and variance differences under RCP4.5 than RCP8.5. For the NEX-GDDP data set, the average differences depict fewer amounts under RCP4.5 than RCP8.5; however, in relation to the Marksim data set the situation is inverted. Even though the Marksim data set overestimates precipitation, the NEX-GDDP data set underestimates it and this underestimation is more than the Marksim's overestimation (Tables 3 and 4).

**Table 2.** The monthly-average observation data in the Lali region during the verification time period (2010-2016).

Month	Pr (mm)	Tmin (°C)	Tmax (°C)
January	81.15	7.51	17.57
February	44.44	8.83	19.53
March	64.91	11.42	23.99
April	35.49	16.51	30.44
May	15.08	23.02	37.55
June	0.01	27.03	43.38
July	0.06	29.77	45.70
August	0.06	29.18	45.04
September	0.86	25.23	41.11
October	15.89	20.21	34.24
November	70.08	13.53	24.61
December	78.04	8.74	19.49
<b>Mean</b>	<b>33.84</b>	<b>18.41</b>	<b>31.89</b>

**Table 3.** The RMSE, average (da=observation average-simulated average) and variance differences (dv=observation variance-simulated variance) between the GCMs' outputs and observation data for precipitation (Pr (mm)), the minimum temperature (Tmin (°C)) and the maximum temperature (Tmax (°C)) considering all GCMs involved in the NEX-GDDP and Marksim data sets under RCP4.5 during the verification time period.

GCMs	NEX-GDDP									Marksim								
	Pr			Tmin			Tmax			Pr			Tmin			Tmax		
	dv	da	RMSE	dv	da	RMSE	dv	da	RMSE	dv	da	RMSE	dv	da	RMSE	dv	da	RMSE
BCC-CSM1-1	-190.3	1.6	18.0	14.1	3.2	3.4	-0.2	1.1	1.5	-199.4	-1.4	11.9	4.3	1.3	1.5	-10.8	-0.9	1.4
CSIRO-MK3-6-0	-233.6	2.2	11.7	9.6	3.5	3.6	-3.9	1.5	1.6	-268.6	-1.9	11.8	3.9	2.0	1.5	-7.9	-0.8	1.3
<b>GFDL-CM3</b>	350.9	6.3	15.4	<b>10.0</b>	<b>3.1</b>	<b>3.3</b>	<b>2.4</b>	<b>0.6</b>	<b>1.1</b>	-141.2	-2.3	10.8	<b>1.8</b>	<b>0.9</b>	<b>1.2</b>	<b>-10.6</b>	<b>-1.4</b>	<b>1.7</b>
GFDL-ESM2G	-132.1	0.9	18.0	16.1	3.1	3.4	5.3	0.8	1.0	-289.0	-2.9	13.9	5.7	1.1	1.4	-8.2	-1.1	1.5
GFDL-ESM2M	-14.9	5.5	16.8	13.3	3.5	3.7	3.9	1.2	1.5	-381.8	-6.4	13.7	7.9	1.7	2.0	-9.0	-0.4	1.1
IPSL-CM5A-LR	625.5	16.0	24.1	16.9	3.0	3.3	8.8	0.7	1.1	-235.8	-0.7	13.8	8.8	0.9	1.3	-4.7	-0.9	1.4
IPSL-CM5A-MR	242.0	12.5	26.3	19.6	2.9	3.3	10.5	0.8	1.2	-283.1	-1.4	12.3	8.0	1.1	1.6	-1.2	-0.9	1.2
MIROC5	241.4	6.1	13.4	5.3	3.3	3.4	-2.0	1.2	1.3	-147.8	-0.7	10.5	2.2	1.1	1.5	-11.5	-1.0	1.6
MIROC-ESM	218.9	5.4	11.8	11.8	3.5	3.6	2.9	1.5	1.7	-155.9	-3.4	12.1	4.0	1.1	1.4	-5.3	-0.7	1.1
MIROC-ESM-CHEM	487.5	10.2	14.5	8.4	3.1	3.2	-2.6	0.8	1.1	-174.1	-4.4	11.2	3.8	0.9	1.4	-6.4	-0.9	1.5
MRI-CGCM3	203.9	5.6	16.7	17.3	3.3	3.5	13.7	1.2	1.6	-138.0	-2.4	10.3	9.6	1.4	1.6	-0.9	-0.6	1.0
<b>NorESM1-M</b>	<b>-18.2</b>	<b>0.8</b>	<b>13.0</b>	11.6	3.3	3.4	-0.7	1.5	1.8	<b>-67.3</b>	<b>0.8</b>	<b>13.3</b>	4.0	1.3	1.7	-4.2	-0.9	1.6
<b>Mean</b>	<b>148.4</b>	<b>6.1</b>	<b>16.6</b>	<b>12.8</b>	<b>3.2</b>	<b>3.4</b>	<b>3.2</b>	<b>1.1</b>	<b>1.4</b>	<b>-207.0</b>	<b>-2.3</b>	<b>12.1</b>	<b>5.3</b>	<b>1.2</b>	<b>1.5</b>	<b>-6.7</b>	<b>-0.9</b>	<b>1.4</b>
ACCESS1-0	91.7	2.4	15.6	5.2	3.2	3.3	-4.5	1.3	1.8	-	-	-	-	-	-	-	-	-
BNU-ESM	436.2	21.1	7.3	8.0	3.2	3.3	-0.8	1.1	1.4	-	-	-	-	-	-	-	-	-
<b>CanESM2</b>	<b>-63.2</b>	<b>-0.4</b>	<b>10.9</b>	13.7	2.8	3.0	5.6	1.0	1.3	-	-	-	-	-	-	-	-	-
CCSM4	81.9	5.4	18.0	12.1	3.1	3.3	4.4	1.0	1.3	-	-	-	-	-	-	-	-	-
CESM1-BGC	387.4	8.5	17.9	17.1	3.2	3.4	10.0	0.9	1.4	-	-	-	-	-	-	-	-	-
CNRM-CM5	-1274.8	-6.0	29.2	10.2	3.1	3.3	-5.6	1.9	2.1	-	-	-	-	-	-	-	-	-
INM-CM4	477.2	-10.1	14.6	13.2	3.9	4.0	5.0	1.7	1.8	-	-	-	-	-	-	-	-	-
MPI-ESM-LR	639.0	12.5	19.8	11.3	2.9	3.1	-0.6	0.8	1.1	-	-	-	-	-	-	-	-	-
MPI-ESM-MR	264.4	5.0	14.5	10.6	2.8	3.0	-3.8	1.0	1.3	-	-	-	-	-	-	-	-	-
<b>Mean</b>	<b>115.6</b>	<b>5.0</b>	<b>18.0</b>	<b>11.3</b>	<b>3.1</b>	<b>3.3</b>	<b>1.1</b>	<b>1.2</b>	<b>1.5</b>	-	-	-	-	-	-	-	-	-
BCC-CSM 1.1(m)	-	-	-	-	-	-	-	-	-	-56.6	-1.4	10.5	1.8	1.1	1.3	-10.3	-1.1	1.5
FIO-ESM	-	-	-	-	-	-	-	-	-	-256.5	-2.4	11.8	5.2	1.6	1.8	-6.1	-0.5	1.2
GISS-E2-H	-	-	-	-	-	-	-	-	-	-377.6	-3.7	13.0	7.5	1.1	1.5	-4.9	-0.6	1.2
GISS-E2-R	-	-	-	-	-	-	-	-	-	-466.5	-8.4	15.7	7.4	1.2	1.5	-5.5	-0.5	1.2
HadGEM2-ES	-	-	-	-	-	-	-	-	-	-362.7	-3.4	13.9	4.8	1.1	1.4	-6.4	-1.2	1.6
<b>Mean</b>	-	-	-	-	-	-	-	-	-	<b>-304.0</b>	<b>-3.9</b>	<b>13.0</b>	<b>5.4</b>	<b>1.2</b>	<b>1.5</b>	<b>-6.6</b>	<b>-0.7</b>	<b>1.3</b>
<b>Total mean</b>	<b>134.3</b>	<b>5.3</b>	<b>16.6</b>	<b>12.2</b>	<b>3.2</b>	<b>3.4</b>	<b>2.3</b>	<b>1.1</b>	<b>1.4</b>	<b>-235.4</b>	<b>-2.7</b>	<b>12.4</b>	<b>5.3</b>	<b>1.2</b>	<b>1.5</b>	<b>-6.7</b>	<b>-0.8</b>	<b>1.4</b>

**Table 4.** The RMSE, average (da=observation average-simulated average) and variance differences (dv=observation variance-simulated variance) between the GCMs' outputs and observation data for precipitation (Pr (mm)), the minimum temperature (Tmin (°C)) and the maximum temperature (Tmax (°C)) considering all GCMs involved in the NEX-GDDP and Marksim data sets under RCP8.5 during the verification time period.

GCMs	NEX-GDDP									Marksim								
	Pr			Tmin			Tmax			Pr			Tmin			Tmax		
	dv	da	RMSE	dv	da	RMSE	dv	da	RMSE	dv	da	RMSE	dv	da	RMSE	dv	da	RMSE
BCC-CSM1-1	212.0	8.1	19.9	5.8	3.0	3.0	-5.1	0.6	1.3	-146.1	1.0	13.7	1.1	1.1	1.4	-8.3	-1.3	1.8
CSIRO-MK3-6-0	305.6	9.8	15.7	4.6	3.4	3.5	-6.9	1.2	1.3	-197.6	-1.0	11.2	3.4	1.2	1.4	-7.1	-0.9	1.3
<b>GFDL-CM3</b>	246.5	8.9	14.8	<b>3.0</b>	<b>2.5</b>	<b>2.7</b>	<b>-6.3</b>	<b>0.3</b>	<b>0.8</b>	-59.4	-1.5	10.5	<b>0.6</b>	<b>0.8</b>	<b>1.4</b>	<b>-11.4</b>	<b>-1.4</b>	<b>1.9</b>
GFDL-ESM2G	246.1	6.5	13.8	9.9	2.8	2.9	-2.4	0.6	1.0	-67.0	1.4	13.7	6.6	1.0	1.4	-5.4	-1.3	1.6
GFDL-ESM2M	369.4	7.9	22.7	9.6	3.6	3.7	1.8	1.2	1.4	-324.6	-2.9	14.7	5.8	1.5	1.7	-7.7	-0.8	1.4
IPSL-CM5A-LR	604.5	14.2	23.1	15.3	3.4	3.6	-0.8	0.8	1.2	-225.4	-0.7	13.0	7.3	0.8	1.3	-3.7	-1.2	1.6
IPSL-CM5A-MR	540.4	13.2	23.0	15.3	3.2	3.4	5.2	0.9	1.4	-269.7	-2.5	12.1	9.6	0.9	1.5	-0.8	-0.9	1.3
MIROC5	212.2	6.6	17.0	7.7	3.5	3.5	-0.9	1.4	1.6	-600.6	-6.1	15.6	5.0	0.7	1.2	-9.6	-1.1	1.5
MIROC-ESM	539.3	9.0	16.4	7.8	3.3	3.4	-0.7	1.0	1.3	-241.1	-5.9	15.4	5.5	1.2	1.4	-3.8	-0.7	1.1
MIROC-ESM-CHEM	-861.3	-3.1	23.8	8.2	2.4	2.6	-7.9	0.7	1.0	-257.5	-3.4	12.5	3.3	1.0	1.4	-10.4	-1.0	1.8
MRI-CGCM3	-108.2	4.0	21.9	14.9	3.5	3.6	6.3	1.3	1.8	-296.5	-3.1	15.8	10.0	1.4	1.7	-0.8	-0.6	1.4
<b>NorESM1-M</b>	<b>178.4</b>	<b>2.5</b>	<b>11.2</b>	9.6	2.9	3.0	4.0	1.0	1.4	<b>-46.2</b>	<b>-1.9</b>	<b>10.8</b>	4.5	1.1	1.5	-3.1	-0.8	1.4
<b>Mean</b>	<b>207.1</b>	<b>7.3</b>	<b>18.6</b>	<b>9.3</b>	<b>3.1</b>	<b>3.3</b>	<b>-1.2</b>	<b>0.9</b>	<b>1.3</b>	<b>-227.6</b>	<b>-2.2</b>	<b>13.2</b>	<b>5.2</b>	<b>1.1</b>	<b>1.5</b>	<b>-6.0</b>	<b>-1.0</b>	<b>1.5</b>
ACCESS1-0	-334.7	9.2	25.0	6.7	3.0	3.1	-3.7	1.2	1.4	-	-	-	-	-	-	-	-	-
BNU-ESM	216.8	7.6	16.4	9.4	2.7	2.9	0.1	0.7	1.0	-	-	-	-	-	-	-	-	-
<b>CanESM2</b>	<b>-94.1</b>	<b>1.6</b>	<b>18.2</b>	8.5	2.6	2.7	0.4	0.6	1.2	-	-	-	-	-	-	-	-	-
CCSM4	367.6	9.1	15.0	8.4	3.3	3.4	-0.7	0.6	0.7	-	-	-	-	-	-	-	-	-
CESM1-BGC	-552.4	-0.4	15.7	10.0	3.1	3.2	-7.9	1.2	1.3	-	-	-	-	-	-	-	-	-
CNRM-CM5	596.6	13.0	20.6	13.0	2.8	3.0	7.6	0.3	0.7	-	-	-	-	-	-	-	-	-
INM-CM4	1.4	0.0	10.8	11.0	3.4	3.6	-1.9	1.6	1.7	-	-	-	-	-	-	-	-	-
MPI-ESM-LR	-41.9	3.6	16.5	13.1	3.0	3.2	3.2	1.1	1.4	-	-	-	-	-	-	-	-	-
MPI-ESM-MR	333.8	8.5	13.7	5.2	3.0	3.0	-10.7	0.9	1.1	-	-	-	-	-	-	-	-	-
<b>Mean</b>	<b>54.8</b>	<b>5.8</b>	<b>16.9</b>	<b>9.4</b>	<b>3.0</b>	<b>3.1</b>	<b>-1.5</b>	<b>0.9</b>	<b>1.2</b>	-	-	-	-	-	-	-	-	-
BCC-CSM 1.1(m)	-	-	-	-	-	-	-	-	-	-3.5	0.1	11.2	4.5	1.0	1.3	-4.2	-1.2	1.6
FIO-ESM	-	-	-	-	-	-	-	-	-	-231.5	-2.9	10.8	7.5	1.5	1.8	-3.1	-0.3	1.0
GISS-E2-H	-	-	-	-	-	-	-	-	-	-505.7	-1.8	14.6	7.6	1.0	1.4	-4.8	-0.9	1.4
GISS-E2-R	-	-	-	-	-	-	-	-	-	-514.8	-7.8	13.9	7.1	1.2	1.5	-4.9	-0.5	1.1
HadGEM2-ES	-	-	-	-	-	-	-	-	-	-246.4	-2.5	12.1	3.9	1.0	1.3	-6.2	-1.3	1.7
<b>Mean</b>	-	-	-	-	-	-	-	-	-	<b>-300.4</b>	<b>-3.0</b>	<b>12.5</b>	<b>6.1</b>	<b>1.1</b>	<b>1.5</b>	<b>-4.7</b>	<b>-0.8</b>	<b>1.4</b>
<b>Total mean</b>	<b>141.8</b>	<b>6.7</b>	<b>17.9</b>	<b>9.4</b>	<b>3.1</b>	<b>3.2</b>	<b>-1.3</b>	<b>0.9</b>	<b>1.2</b>	<b>-249.0</b>	<b>-2.5</b>	<b>13.0</b>	<b>5.5</b>	<b>1.1</b>	<b>1.5</b>	<b>-5.6</b>	<b>-0.9</b>	<b>1.5</b>

The NEX-GDDP data set demonstrates better operation criteria than the Marksim data set by considering all GCMs whether in common

or not as an ensemble under both RCPs. In other words, for the NEX-GDDP data set the common GCMs have higher RMSE, average

and variance differences than uncommon GCMs, and for the Marksim data set the situation is the antithesis of the NEX-GDDP data set.

In relation to precipitation, NorESM1-M has the fewest values of RMSE, average and variance differences, i.e. the best operation criteria, in comparison with the other GCMs in both NEX-GDDP and Marksim data sets.

The outputs of model NorESM1-M in the Marksim data set indicate more precipitation, especially for the wet months, in the future time period than the present/historical time period under both scenarios. The present/historical time period is only available for the NEX-GDDP data set. The outputs of model NorESM1-M in the NEX-GDDP data set approximately depict lower precipitation in winter (January to March) and more precipitation in autumn (October to December) in the future time period than the present/historical time period under both scenarios. NorESM1-M outputs of precipitation for the Marksim data set are approximately smoother than the NEX-GDDP data set under both scenarios. Finally, the model, in both data sets, has projected higher precipitation under RCP4.5 than RCP8.5 during the early months of the year; however, during the late months of the year the situation is exactly the opposite (Figure 2).

Even though the NEX-GDDP GCMs operate

better for the maximum temperature than the minimum temperature, the Marksim GCMs operate almost the same for both of them. Considering the operation criteria for the Marksim GCMs makes it obvious that GFDL-CM3 has the best operation to project the minimum temperature under both RCPs. Moreover, considering the operation criteria in both data sets makes it obvious that the maximum temperature is projected better by the NEX-GDDP GCMs than the Marksim GCMs, especially by considering the variance differences. On the other side, the minimum temperature is projected better by the Marksim GCMs than the NEX-GDDP GCMs (Tables 3 and 4).

In conclusion, in relation to the minimum and maximum temperatures, the best GCM was selected among the Marksim and NEX-GDDP GCMs, respectively, which is GFDL-CM3 for both minimum and maximum temperatures.

The minimum and maximum temperatures would escalate in the Lali region during the future time period than the present/historical time period. This temperature escalation is demonstrated by both NEX-GDDP and Marksim data sets; however, the Marksim data set depicts more temperature increment than the NEX-GDDP data set. Finally, the minimum and maximum temperatures demonstrate slightly more augmentation under RCP8.5 than RCP4.5 (Figures 3 and 4).

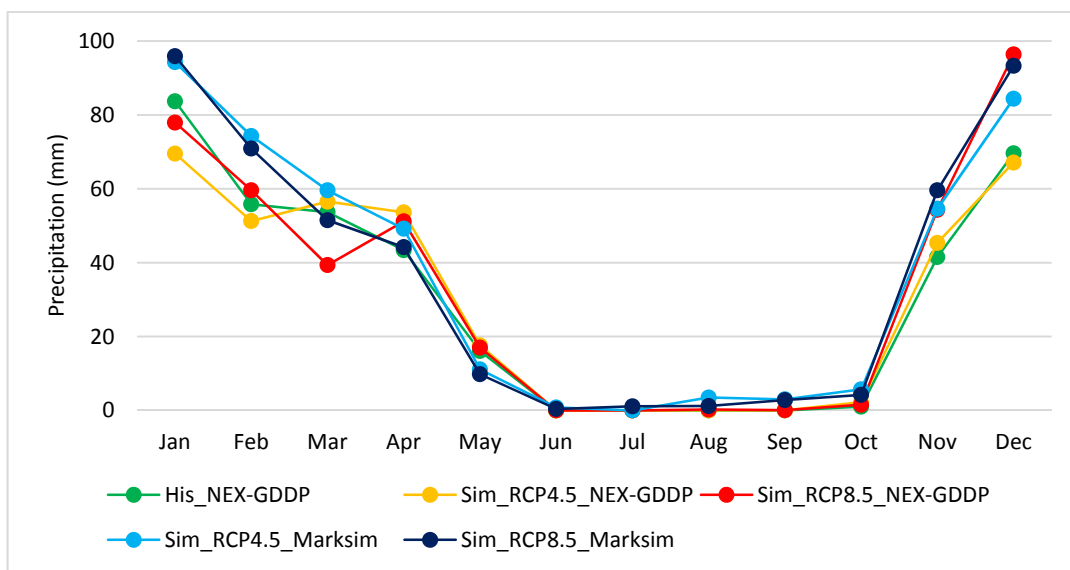


Figure 2. Projection of the monthly-average precipitation by NorESM1-M in the NEX-GDDP and Marksim data sets under RCP4.5 and RCP8.5 for the present/historical (His) and future (Sim) time periods.

Table 5 demonstrates the values and changes of precipitation, the minimum temperature, and the maximum temperature for both data sets and emission scenarios using NorESM1-M for precipitation and GFDL-CM3 for the minimum and maximum temperatures in the future time period than the present/historical time period.

Precipitation would probably change between -0.40 and +9 % using the selected model and the NEX-GDDP data set, and +19.20 and +20.73 % using the selected model and the Marksim data set in the future time period than the present/historical time period. The minimum temperature would probably variate between +2.25 and

+2.89°C using the selected model and the NEX-GDDP data set, and +4.24 and +4.78°C using the selected model and the Marksim data set in the future time period than the present/historical time period. The maximum temperature would probably variate between +3.12 and +3.71°C using the selected model and the NEX-GDDP data set, and +5.08 and +5.58°C using the selected model and the Marksim data set in the future time period than the present/historical time period. As indicated previously, the minimum temperature and the maximum temperature were simulated better by the Marksim dataset and the NEX-GDDP data set, respectively.

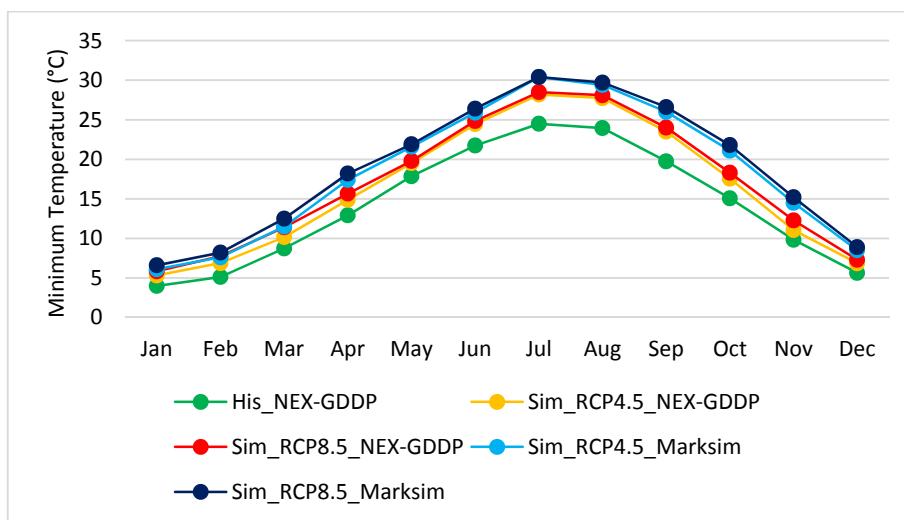


Figure 3. Projection of the monthly-average minimum temperature by GFDL-CM3 in the NEX-GDDP and Marksim data sets under RCP4.5 and RCP8.5 for the present/historical (His) and future (Sim) time periods.

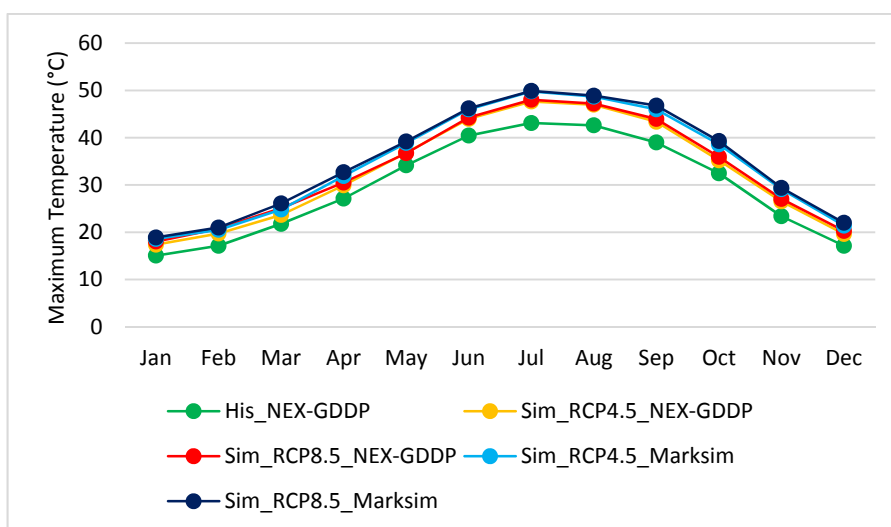


Figure 4. Projection of the monthly-average maximum temperature by GFDL-CM3 in the NEX-GDDP and Marksim data sets under RCP4.5 and RCP8.5 for the present/historical (His) and future (Sim) time periods.

**Table 5.** Precipitation, the minimum and maximum temperatures values and changes in the NEX-GDDP and Marksim data sets under RCP4.5 and RCP8.5 using NorESM1-M for precipitation and GFDL-CM3 for the minimum and maximum temperatures in the present/historical (His) and future (Sim) time periods.

Variable	Value/change	NEX-GDDP			Marksim	
		His	Sim_RCP4.5	Sim_RCP8.5	Sim_RCP4.5	Sim_RCP8.5
Precipitation	Value (mm)	30.4	30.28	33.14	36.71	36.24
	Change (%)	-	-0.4	9	20.73	19.2
The minimum temperature	Value (°C)	14.09	16.34	16.98	18.33	18.87
	Change (°C)	-	2.25	2.89	4.24	4.78
The maximum temperature	Value (°C)	29.45	32.57	33.16	34.52	35.03
	Change (°C)	-	3.12	3.71	5.08	5.58

Enhancement of precipitation in the Lali region during some months of the year in the future time period than the present/historical time period may not improve hydrological or agricultural circumstances due to increments of the minimum and maximum temperatures.

#### 4. Discussion

The operation of GCMs in relation to precipitation is inferior to the minimum and maximum temperatures in the Lali region (Tables 3 and 4). As a matter of fact, the correlation of precipitation is not without vicissitudes and it is a two-part model. One part determines whether it precipitates or not, and the other calculates the amount of precipitation. The last is controlled strongly by the air masses and local conditions. In actuality, precipitation does not follow any weather principles such as the air masses and topography in the Lali region. It is definitely difficult to find the diurnal correlation of precipitation in the arid areas since there is no precipitation at most days such that if a rainy day differs or does not match, the correlation will be zero. Further, precipitation does not have normal distribution. Indeed, it is recommended to employ the monthly averages and variances whether as the average or sum of monthly precipitation; thence, the normal distribution would be more probable (<http://gismap.ciat.cgiar.org/MarksimGCM/docs/FAQ.html>).

GCMs in both data sets under both RCPs overestimate the minimum temperature in the Lali region (Tables 3 and 4). Even though the NEX-GDDP data set under both RCPs overestimates the maximum temperature, the Marksim data set under both RCPs

underestimates it in the Lali region. Indeed, most GCMs overestimate the average temperature over Northern Eurasia (Miao et al., 2014), the Arctic (Chylek et al., 2011), the Northern hemisphere (Zhao et al., 2013) and even in the world (Kim et al., 2012). The stratospheric aerosol concentration's enhancement due to the volcanos' eruptions has lowered the temperature significantly during the recent years. This has not been considered in the GCMs' structures (Santer et al., 2014; Solomon et al., 2011).

By considering the GCMs' outputs in both data sets, it is not recondite that the GCMs with higher resolutions do not imperatively demonstrate better projections than the GCMs with lower resolutions. NorESM1-M and GFDL-CM3 depicted the best results in the Lali region even though they do not have the highest resolutions (Table 1). Furthermore, the outputs of the uncommon GCMs demonstrate the ability of some GCMs in projecting the climatic variables. For instance, CanESM2 in the NEX-GDDP data set illustrates satisfactory results.

The selected models were chosen by considering the operation criteria of the GCMs in both data sets. The results of this study have been reached by considering only seven years of the observation data (2010-2016); however, had longer observations been taken into account, different results may have been achieved. The other point is that different results may be achieved for other regions.

Yoo and Cho (2018) evaluated the performance of 20 GCMs in CMIP5 from the World Data Center for Climate (WDCC) as global, zonal and grid mean data structures. They employed different GCMs with

different grid resolutions, including NCAR-CAM5 (1.250° × 0.938°) to IPSL-CM5A-LR (3.750° × 1.875°). However, NorESM1-M, as in the case of the Lali region, demonstrated the best performance according to the criteria like the RMSE considering the Global Precipitation Climatology Project (GPCP) data as the observation data in the time period 2006-2014. They additionally declared that the RMSE can disclose the average differences and standard deviations; therefore, it can be an appropriate criterion for the evaluation of the GCMs' predictions.

Figures 5 and 6 illustrate the radar chart demonstrating the RMSE of the common models in the NEX-GDDP and Marksim data sets under both scenarios for precipitation and the average temperature. The Marksim's GCMs demonstrate lower RMSE than the NEX-GDDP dataset for precipitation and the average temperature. Further, the RMSE of both data sets are moderately lower under RCP4.5 than RCP8.5. NorESM1-M portrays the best results for precipitation (Figure 5). In relation to the average temperature, not only does GFDL-CM3 represent the appropriate ability, but also MIROC-ESM-CHEM portrays capability (Figure 6). However,

GFDL-CM3 outperforms MIROC-ESM-CHEM since the mean of the variance differences for GFDL-CM3 and MIROC-ESM-CHEM are 5.77 and 6.38, respectively. The emission scenarios may be the source of uncertainty; however, the error originated from the GCMs is more than the uncertainty derived from the emission scenarios (Daksiya et al., 2017). If other emission scenarios, i.e. RCP2.6 and RCP6, Had been included in the NEX-GDDP data set, interpreting of their projections could have been included and it may have eventuated in some satisfactory results.

A multi-model ensemble includes many models produced by different research modelling centers in the world. However, the models' outputs approximately correlate in a multi-model ensemble due to initially, the similarity between the dynamical cores and the physical parameterizations and secondly, the same observation data included in them. Indeed, they constitute a cluster in relation to the simulation of climate change (Knutti et al., 2013; Masson and Knutti, 2011). The reader may consult Zubler et al. (2016) to obtain more information about the number of select possibilities from an ensemble point of view.

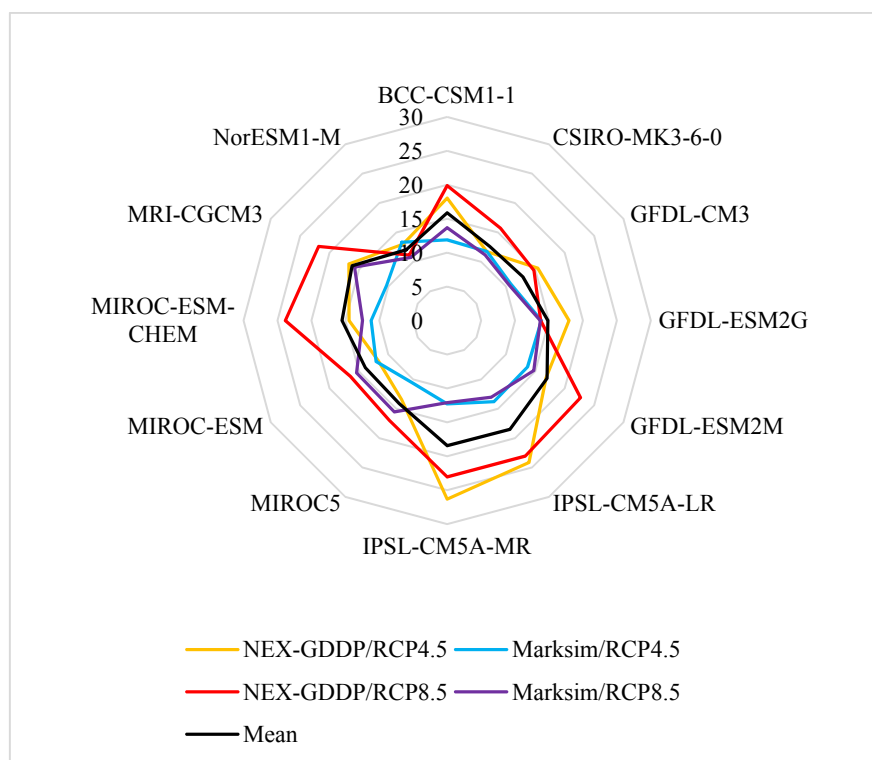
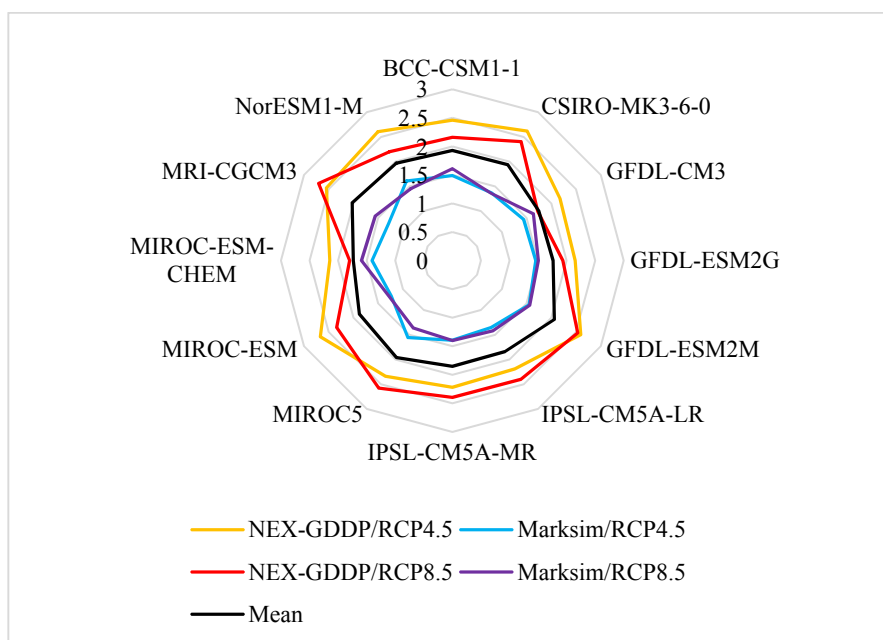


Figure 5. Radar chart demonstrating the RMSE of the common models in the NEX-GDDP and Marksim data sets under RCP4.5 and RCP8.5 for precipitation.



**Figure 6.** Radar chart demonstrating the RMSE of the common models in the NEX-GDDP and Marksim data sets under RCP4.5 and RCP8.5 for the average temperature.

IPCC (2013) stated ‘one model one vote’ and recommended considering all GCMs together. It is a challenge to determine unsatisfactory GCMs so that the relationship between the poor performance of the GCMs and the future projection of them is nebulous. McSweeney et al. (2015) cited some studies with down-weighting or exclusion of GCMs. Some authors like Overland et al. (2011) stated that not considering the unsatisfactory GCMs may reduce the uncertainties. In this study, in relation to the climate change impacts on the Lali region, which is a small-scale study, the best models were selected and then, precipitation and temperature were projected according to the selected models in the future time period.

Overland et al. (2011) and McSweeney et al. (2012) declared that selecting the best GCMs/GCM and removing the worst GCMs/GCM may be more accurate in the local studies, like the Lali region, than the regional (or large-scale) studies because the integral characteristics of the GCMs may be abundantly transparent in the local studies.

The GCM selection process may be a key aspect exerting a powerful influence on the results. In this study, some statistical criteria like the RMSE have been employed; however, other approaches like McSweeney et al. (2015) may have been applied.

Unfortunately, no standardized criterion exists for the GCM selection process in the literature (Nyunt et al., 2016).

Evans (2009) evaluated the Middle East under climate change during the 21<sup>st</sup> century using the outputs of 18 GCMs under the A2 emission scenario. The temperature demonstrated an escalation of 1.4 and 4K for the middle and late of the century, respectively. Even though precipitation depicted a reduction over the area, it portrayed an augmentation in a few areas, including the Lali region. Further, the performance of various GCMs was assessed. BCC and PCM had the most biases for precipitation and temperature, respectively, and CCSM, MIUB and MRI had the best performance for precipitation. This study was carried out in a regional scale over the Middle East, and for a specific region, like the Lali region, it is recommended to downscale the outputs of the GCMs to obtain detailed information. The downscaled outputs of different GCMs in the Lali region acknowledge the mentioned study.

Nassery and Salami (2016) evaluated 16 GCMs based on the weighting approach in Hamadan aquifer, west Iran and selected CGCM2.3.2a and HadCM3 as the best models in relation to precipitation and temperature, respectively. They employed

LARS-WG for downscaling and concluded that temperature would ascend about 1.4°C, and precipitation and runoff would change from -6 to +10 % and from -39 to +12 % both under A2 and B1 emission scenarios, respectively. Moreover, Samadi et al. (2010) applied the regression and some functional standards (RMSE, R2 and MAE) to evaluate the performance of some GCMs in Kermanshah synoptic station, west Iran. They demonstrated that HadCM3 operates the best in projecting the climatic variables, i.e. precipitation and temperature, in the study area. However, CGCM2.3.2a and HadCM3 are not included in both NEX-GDDP and Marksim data sets to assess their operations in the Lali region.

The NEX-GDDP and Marksim data sets have been employed in various studies without any statistical corrections (Bao and Wen, 2017; Chen et al., 2017; Daksiya et al., 2017; Jones and Thornton, 2013).

Even though the Marksim data set has been utilized globally (Bharati et al., 2014; De Trincheria et al., 2015; Rao et al., 2015), little peer-reviewed literature has considered its evaluation and verification. However, it has been assessed in some studies (Kahimba et al., 2014; Mavromatis and Hansen, 2001; Mzirai et al., 2005), and the results have demonstrated the proven ability of this data set. However, some results have revealed a relatively poor operation of this data set in the reproduction of the inter-annual variability so that in some regions it may not operate as well as the other weather generators. One of the issues is that the precipitation variances are underestimated by this data set although this problem would be dissolved by resampling of the probable Markov coefficients (Jones, 2013).

## 5. Conclusions

Nowadays, some downscaled climatic data sets exist that enhance the ability to employ the climatic data worldwide even in the regions with little synoptic data, like the Lali region. In this study, the power of different GCMs in projecting the climate change impacts on the Lali region was characterized by taking into account some statistical criteria. Even though the NEX-GDDP and Marksim data sets may be utilized globally, it is recommended to employ the Marksim data

set for the minimum temperature and the NEX-GDDP data set for the maximum temperature in the Lali region. In the case of precipitation, the NEX-GDDP data set demonstrated better results by considering the variance differences while the Marksim data set portrayed better results by considering the RMSE and the average differences in the Lali region. NorESM1-M and GFDL-CM3 depicted the best results for precipitation and temperature, whether the minimum temperature or the maximum temperature, respectively. The results of the selected GCM for the temperature represented warming of the Lali region. The results of the selected GCM for precipitation illustrated its increment using the Marksim data set, its decrement during the early months of the year, and its increment during the late months of the year using the NEX-GDDP data set. While more precipitation was simulated by the GCMs under RCP4.5 than RCP8.5 for both data sets in the winter, RCP8.5 illustrated more precipitation for the late months of the year. Generally, higher precipitation and temperature, either the minimum temperature or the maximum temperature, were projected by the Marksim data set than the NEX-GDDP dataset in the Lali region.

## References

- Bao, Y. and Wen, X., 2017, Projection of China's near- and long-term climate in a new high-resolution daily downscaled data set NEX-GDDP, *J. Meteorol. Res.*, 31(1), 236-249.
- Bharati, L., Gurung, P., Jayakody, P., Smakhtin, V. and Bhattarai, U., 2014, The projected impact of climate change on water availability and development in the Koshi Basin, Nepal, *Mt. Res. Dev.*, 34(2), 118-130.
- Chaturvedi, R. K., Joshi, J., Jayaraman, M., Bala, G. and Ravindranath, N., 2012, Multi-model climate change projections for India under representative concentration pathways, *Curr. Sci.*, 103(7), 791-802.
- Chen, H. P., Sun, J. Q. and Li, H. X., 2017, Future changes in precipitation extremes over China using the NEX-GDDP high-resolution daily downscaled data-set, *Atmos. Ocean. Sci. Lett.*, 10(6), 403-410.

- Chen, H., Sun, J. and Chen, X., 2014, Projection and uncertainty analysis of global precipitation-related extremes using CMIP5 models, *Int. J. Climatol.*, 34(8), 2730-2748.
- Chou, S. C., Lyra, A., Mourão, C., Dereczynski, C., Pilotto, I., Gomes, J., Bustamante, J., Tavares, P., Silva, A., Rodrigues, D., Campos, D., Chagas, D., Sueiro, G., Siqueira, G., Nobre, P. and Marengo, J., 2014, Assessment of climate change over South America under RCP 4.5 and 8.5 downscaling scenarios, *Am. J. of Clim. Change*, 3(5), 512-525.
- Chylek, P., Li, J., Dubey, M., Wang, M. and Lesins, G., 2011, Observed and model simulated 20th century Arctic temperature variability: Canadian earth system model CanESM2, *Atmos. Chem. Phys.*, 8, 22893-22907.
- Daksiya, V., Mandapaka, P. and Lo, E. Y., 2017, A Comparative Frequency Analysis of Maximum Daily Rainfall for a SE Asian Region under Current and Future Climate Conditions, *Adv. Meteorol.*, 2, 1-16.
- De Trincheria, J., Craufurd, P., Harris, D., Mannke, F., Nyamangara, J., Rao, K. and Leal Filho, W., 2015, Adapting agriculture to climate change by developing promising strategies using analogue locations in eastern and southern Africa: a systematic approach to develop practical solutions, in: Leal Filho, W., Esilaba, A., Rao, K. and Sridhar, G. (Eds.), *Adapting African Agriculture to Climate Change*, Climate Change Management, Springer, Cham, pp. 1-23.
- Evans, J. P., 2009, 21st century climate change in the Middle East, *Clim. Change*, 92(3-4), 417-432.
- Funk, C., Michaelsen, J. and Marshall, M., 2010, Mapping recent decadal climate variations in Eastern Africa and the Sahel, in: Wardlow, B. D., Anderson, M. C. and Verdin, J. P. (Eds.), *Remote Sensing of Drought: Innovative Monitoring Approaches*, CRC Press, pp. 331-358.
- Geng, S., Auburn, J., Brandstetter, E. and Li, B., 1988, A Program to Simulate Meteorological Variables: Documentation for SIMMETEO, University of California, Agricultural Experiment Station, Davis.
- Hijmans, R. J., Cameron, S. E., Parra, J. L., Jones, P. G. and Jarvis, A. J. I., 2005, Very high resolution interpolated climate surfaces for global land areas, *Int. J. Climatol.*, 25(15), 1965-1978.  
<https://cds.nccs.nasa.gov/nex-gddp/>  
<http://gisweb.ciat.cgiar.org/MarksimGCM/docs/FAQ.html>  
<http://gisweb.ciat.cgiar.org/MarkSimGCM/docs/doc.html>
- Hutchinson, M. F., 1997, ANUSPLIN Version 3.2 User's Guide, The Australian National University, Centre for Resource and Environmental Studies, Canberra, Australia.
- IPCC, 2013, *Climate Change 2013: The Physical Science Basis. Contribution of Working Group I to the Fifth Assessment Report of the Intergovernmental Panel on Climate Change*, in: Stocker, T. F., Qin, D., Plattner, G. K., Tignor, M., Allen, S. K., Boschung, J. et al. (Eds.), Cambridge University Press, Cambridge, UK and New York, USA.
- IPCC, 2014, *Climate Change 2014: Synthesis Report. Contribution of Working Groups I, II and III to the Fifth assessment report of the intergovernmental panel on climate change*, in: Core Writing Team, Pachauri, R. K. and Meyer, L. A. (Eds.), IPCC, Geneva, Switzerland.
- Iran Meteorological Organization, 2018, Climate data including daily precipitation, temperature and solar radiation for Lali synoptic station for 2007-2016 in Excel Format.
- Jones, P. G., 2013, *MarkSim Standalone for DSSAT Users*. International Center for Tropical Agriculture (CIAT), Cali, Colombia.
- Jones, P. G. and Thornton, P. K., 2013, Generating downscaled weather data from a suite of climate models for agricultural modelling applications, *Agr. Sys.*, 114, 1-5.
- Kahimba, F., Tumbo, S., Mpeti, E., Yonah, I., Timiza, W. and Mbungu, W., 2014, Accuracy of Giovanni and Marksim software packages for generating daily rainfall data in selected bimodal climatic areas in Tanzania, *Tanz. J. Agr. Sci.*, 13(1), 12-25.
- Kim, H. M., Webster, P. J. and Curry, J. A., 2012, Evaluation of short-term climate

- change prediction in multi-model CMIP5 decadal hindcasts, *Geophys. Res. Lett.*, 39(10), 1-7.
- Knutti, R., Masson, D. and Gettelman, A., 2013, Climate model genealogy: Generation CMIP5 and how we got there, *Geophys. Res. Lett.*, 40(6), 1194-1199.
- Kundzewicz, Z. W., Mata, L. J., Arnell N. W., Doll, P., Kabat, P., Jimenez, B., Miller, K. A., Oki, T., Sen, Z. and Shiklomanov, I. A., 2007, Freshwater resources and their management, in: Parry, M. L., Canziani, O. F., Palutikof, J. P., van der Linden, P. J. and Hanson, C. E. (Eds.), *Climate Change 2007: Impacts, Adaptation and Vulnerability*, Contribution of Working Group 11 to the Fourth Assessment Report of the Intergovernmental Panel on Climate Change, Cambridge University Press, Cambridge, UK and New York, USA, pp. 173-210.
- Ma, C., Pan, S., Wang, G., Liao, Y. and Xu, Y. P., 2016, Changes in precipitation and temperature in Xiangjiang River Basin, China, *Theor. appl. climatol.*, 123(3-4), 859-871.
- Masson, D. and Knutti, R., 2011, Spatial-scale dependence of climate model performance in the CMIP3 ensemble, *J. Climate*, 24(11), 2680-2692.
- Maurer, E. P. and Hidalgo, H. G., 2008, Utility of daily vs. monthly large-scale climate data: an intercomparison of two statistical downscaling methods, *Hydrol. Earth. Syst. Sci.*, 12, 551-563.
- Mavromatis, T. and Hansen, J. W., 2001, Interannual variability characteristics and simulated crop response of four stochastic weather generators, *Agr. Forest Meteorol.*, 109(4), 283-296.
- McSweeney, C., Jones, R., Lee, R. W. and Rowell, D., 2015, Selecting CMIP5 GCMs for downscaling over multiple regions, *Clim. Dynam.*, 44(11-12), 3237-3260.
- McSweeney, C. F., Jones, R. G. and Booth, B. B., 2012, Selecting ensemble members to provide regional climate change information, *J. Climate*, 25(20), 7100-7121.
- Meinshausen, M., Smith, S. J., Calvin, K., Daniel, J. S., Kainuma, M., Lamarque, J. F., Matsumoto, K., Montzka, S. A., Raper, S. C. B., Riahi, K., Thomson, A., Velders, G. J. M. and van Vuuren D. P. P., 2011, The RCP greenhouse gas concentrations and their extensions from 1765 to 2300, *Clim. Change*, 109, 213-241.
- Miao, C., Duan, Q., Sun, Q., Huang, Y., Kong, D., Yang, T., Ye, A., Di, Z. and Gong, W., 2014, Assessment of CMIP5 climate models and projected temperature changes over Northern Eurasia, *Environ. Res. Lett.*, 9(5), 1-12.
- Mohanty, M., Sinha, N. K., Hati, K., Chaudhary, R. and Patra, A., 2015, *Crop Growth Simulation Modelling and Climate Change*, Scientific Publishers, India.
- Mzirai, O., Tumbo, S., Bwana, T., Hatibu, N., Rwehumbiza, F. and Gowing, J., 2005, Evaluation of simulator of missing weather data (SMWD) required in simulation of agro hydrological modeling in the catchment and basin level: case of the PARCHED-THIRST and Marksim Model, *Proceedings of the International Water Management Institute Conference Papers*, Santiago, Chile.
- Nassery, H. and Salami, H., 2016, Identifying vulnerable areas of aquifer under future climate change (case study: Hamadan aquifer, West Iran), *Arab. J. Geosci.*, 9(8), 1-16.
- Nyunt, C. T., Koike, T. and Yamamoto, A., 2016, Statistical bias correction for climate change impact on the basin scale precipitation in Sri Lanka, Philippines, Japan and Tunisia, *Hydrol. Earth Syst. Sci. Discuss.* doi: 10.5194/hess-2016-14
- Overland, J. E., Wang, M., Bond, N. A., Walsh, J. E., Kattsov, V. M. and Chapman, W. L. 2011, Considerations in the selection of global climate models for regional climate projections: The Arctic as a case study, *J. Climate*, 24(6), 1583-1597.
- Rao, M. S., Swathi, P., Rao, C. A. R., Rao, K., Raju, B., Srinivas, K., Manimanjari, D. and Maheswari, M., 2015, Model and scenario variations in predicted number of generations of *Spodoptera litura* Fab. on peanut during future climate change scenario, *PloS one*, 10(2), 1-12.
- Samadi, S., Sagarwar, G. and Tajiki, M., 2010, Comparison of general circulation

- models: methodology for selecting the best GCM in Kermanshah Synoptic Station, Iran, *Int. J. Global Warm.*, 2(4), 347-365.
- Santer, B. D., Bonfils, C., Painter, J. F., Zelinka, M. D., Mears, C., Solomon, S., Schmidt, G. A., Fyfe, J. C., Cole, J. N. S., Nazarenko, L., Taylor, K. E. and Wentz, F. J., 2014, Volcanic contribution to decadal changes in tropospheric temperature, *Nat. Geosci.*, 7(3), 185-189.
- Semenov, M. A. and Stratonovitch, P., 2015, Adapting wheat ideotypes for climate change: accounting for uncertainties in CMIP5 climate projections, *Climate Res.*, 65, 123-139.
- Sheffield, J., Goteti, G. and Wood, E. F., 2006, Development of a 50-year high-resolution global data set of meteorological forcings for land surface modeling, *J. Climate*, 19(13), 3088-3111.
- Solomon, S., Daniel, J. S., Neely, R. R., Vernier, J. P., Dutton, E. G. and Thomason, L. W., 2011, The persistently variable background stratospheric aerosol layer and global climate change, *Science*, 333(6044), 866-870.
- Taylor, K. E., Stouffer, R. J. and Meehl, G. A., 2012, An overview of CMIP5 and the experiment design, *B. Am. Meteorol. Soc.*, 93(4), 485-498.
- Thrasher, B., Maurer, E. P., McKellar, C. and Duffy, P. B., 2012, Technical Note: Bias correcting climate model simulated daily temperature extremes with quantile mapping, *Hydrol. Earth Syst. Sci.*, 16, 3309-3314.
- Thrasher, B. and Nemani, R., 2015, Nasa earth exchange global daily downscaled projections (nex-gddp), NASA, Washington, D.C., USA.
- Trotochaud, J., Flanagan, D. C. and Engel, B. A., 2016, A simple technique for obtaining future climate data inputs for natural resource models, *Appl. Eng. Agric.*, 32(3), 371-381.
- Ul Hasson, S., Pascale, S., Lucarini, V. and Böhner, J., 2016, Seasonal cycle of precipitation over major river basins in South and Southeast Asia: a review of the CMIP5 climate models data for present climate and future climate projections, *Atmos. Res.*, 180, 42-63.
- Washington, R., Harrison, M., Conway, D., Black, E., Challinor, A., Grimes, D., Jones, R., Morse, A., Kay, G. and Todd, M., 2006, African climate change: taking the shorter route, *B. Am. Meteorol. Soc.*, 87(10), 1355-1366.
- Wilby, R. L., 2007, Decadal Forecasting Techniques for Adaptation and Development Planning: A Briefing Document on Available Methods, Constraints, Risks and Opportunities, UK Department for International Development, London.
- Wilby, R. L., Charles, S., Zorita, E., Timbal, B., Whetton, P. and Mearns, L., 2004, Guidelines for Use of Climate Scenarios Developed from Statistical Downscaling Methods, Supporting Material of the Intergovernmental Panel on Climate Change.
- Wilby, R. L., Troni, J., Biot, Y., Tedd, L., Hewitson, B. C., Smith, D. M. and Sutton, R. T., 2009, A review of climate risk information for adaptation and development planning, *Int. J. Climatol.*, 29(9), 1193-1215.
- Wilby, R. L. and Wigley, T., 1997, Downscaling general circulation model output: a review of methods and limitations, *Prog. Phys. Geog.*, 21(4), 530-548.
- Wood, A. W., Leung, L. R., Sridhar, V. and Lettenmaier, D. J., 2004, Hydrologic implications of dynamical and statistical approaches to downscaling climate model outputs, *Clim. Change*, 62(1-3), 189-216.
- Yoo, C. and Cho, E., 2018, Comparison of GCM precipitation predictions with their RMSEs and pattern correlation coefficients, *Water*, 10(1), 1-17.
- Zhao, L., Xu, J. and Powell J. A., 2013, Discrepancies of surface temperature trends in the CMIP5 simulations and observations on the global and regional scales, *Clim. Past*, 6, 6161-6178.
- Zubler, E. M., Fischer, A. M., Fröb, F. and Liniger, M. A., 2016, Climate change signals of CMIP5 general circulation models over the Alps—impact of model selection, *Int. J. Climatol.*, 36(8), 3088-3104.